

# Mutations in the $\alpha 3$ subunit of the vacuolar $H^+$ -ATPase cause infantile malignant osteopetrosis

Uwe Kornak, Ansgar Schulz<sup>1</sup>, Wilhelm Friedrich<sup>1</sup>, Siegfried Uhlhaas<sup>2</sup>, Bernhard Kremens<sup>3</sup>, Thomas Voit<sup>3</sup>, Carola Hasan<sup>4</sup>, Udo Bode<sup>4</sup>, Thomas J. Jentsch<sup>+</sup> and Christian Kubisch<sup>2</sup>

Zentrum für Molekulare Neurobiologie Hamburg, Martinistrasse 85, ZMNH, Universität Hamburg, D-20246 Hamburg, Germany, <sup>1</sup>Universitätskinderklinik, Universität Ulm, D-89075 Ulm, Germany, <sup>2</sup>Institut für Humangenetik, Universität Bonn, D-53111 Bonn, Germany, <sup>3</sup>Klinik und Poliklinik für Kinder- und Jugendmedizin, Universität-Gesamthochschule Essen, D-45122 Essen, Germany and <sup>4</sup>Zentrum für Kinderheilkunde, Universität Bonn, D-53113 Bonn, Germany

Received 23 May 2000; Revised and Accepted 21 June 2000

**Although the gene defects for several mouse mutants with severe osteopetrosis are known, the genes underlying human infantile malignant recessive osteopetrosis remain elusive. Osteopetrosis is thought to be caused by a defect in osteoclast function. These cells degrade bone material in a tightly sealed extracellular compartment that is acidified by a vacuolar (V)-type  $H^+$ -ATPase. Genes encoding components of the acidification machinery are candidate genes for osteopetrosis. In five of ten patients with infantile malignant osteopetrosis, we now demonstrate five different mutations in *OC116*, the gene encoding the  $\alpha 3$  subunit of the V-ATPase from osteoclasts. Two independent patients were homozygous for mutations that predict a total loss of function by severely truncating the protein. By affecting a splice site, another homozygous mutation deletes 14 amino acids within the N-terminus, which interacts with other subunits of the proton pump. On the other hand, in four patients no mutations were found, and one patient from a consanguineous family did not show homozygosity at the *OC116* locus, suggesting that mutations in at least one different gene may underlie osteopetrosis. Our work shows that mutations in the gene encoding the  $\alpha 3$  subunit of the proton pump are a rather common cause of infantile osteopetrosis and suggests that this disease is genetically heterogeneous.**

## INTRODUCTION

Infantile malignant osteopetrosis is a rare autosomal recessive disease which becomes apparent during the first months of life. It is caused by a failure of osteoclasts to resorb bone. Clinical findings include osteosclerosis, hepatosplenomegaly and pancytopenia. It is often associated with visual impairment and hearing loss. This is mostly attributed to cranial nerve compression (1,2), but may also be due to a primary degenera-

tion in some cases (3). The only available treatment is bone marrow transplantation (4). Without treatment, life expectancy rarely exceeds 20 years. Although the gene defects for several osteopetrotic mouse mutants are known (5–7) (reviewed in ref. 8), the only currently known genetic cause of human osteopetrosis are mutations in the carbonic anhydrase II gene (9). In those cases, osteopetrosis is much milder than in infantile malignant osteopetrosis and is associated with renal tubular acidosis. Although a disruption of *src* in mice causes osteopetrosis, attempts to identify mutations in human patients have not been successful (10,11). This also applies for the gene encoding M-SCF which causes osteopetrosis in the *op* mouse (5,12).

Osteoclasts use a vacuolar-type (V-type)  $H^+$ -ATPase to acidify a tightly sealed extracellular compartment between the ruffled border membrane and the bone surface (13). The low pH is necessary both for dissolving inorganic bone material, and for the optimal function of proteases that degrade the organic bone matrix (14). V-type proton ATPases (reviewed in ref. 15) also acidify various intracellular compartments in nearly all cells. This includes lysosomes and vesicles of the secretory and endocytotic pathways. Thirteen subunits of the multimeric  $H^+$ -ATPase protein complex have been isolated. Some of those subunits have several isoforms that show differential tissue distribution. Recently, a new isoform of the membrane-spanning  $\alpha$ -subunit was cloned (16). It was thought to be specific for osteoclasts. Although more recent data show that this isoform, now named  $\alpha 3$ , is not osteoclast-specific, it is induced on osteoclast differentiation and is localized close to the ruffled border under cell culture conditions (17).

*OC116*, the gene encoding the human  $\alpha 3$   $H^+$ -ATPase subunit, was recently mapped to 11q13 (18). A locus for infantile malignant osteopetrosis had already been mapped to this region (19). Importantly, the disruption of the mouse gene (*Atp6i*) encoding the  $\alpha 3$  proton pump subunit caused an osteopetrotic phenotype (20), and the osteopetrotic *oc* mouse model has a mutation in exactly that gene (7). Thus, we considered *OC116* to be an excellent candidate gene for human osteopetrosis.

<sup>+</sup>To whom correspondence should be addressed. Tel: +49 40 42803 4741; Fax: +49 40 42803 4839; Email: jentsch@plexus.uke.uni-hamburg.de

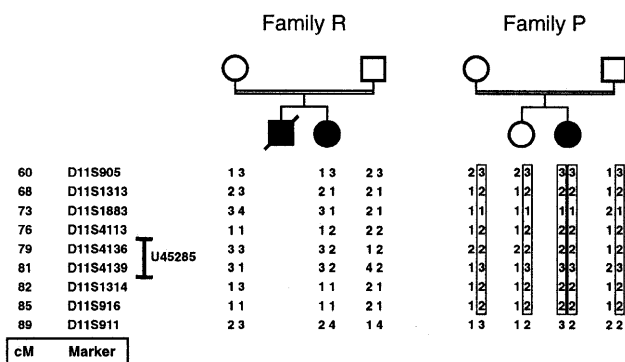


**Figure 1.** Haplotype analysis of two consanguineous families provides evidence for locus heterogeneity in autosomal recessive osteopetrosis. The map location on the left indicates the position of the marker in centimorgans based on the Genethon genetic map (28). The most probable localization of the sequence tagged site marker *U45285* which contains a portion of the *OC116* gene is indicated by the vertical bar and is deduced from the GeneMap'99 (<http://www.ncbi.nlm.nih.gov/genemap/>). In patient R (from a consanguineous Kuwaiti family) the haplotype diverges in the *OC116* region, whereas patient P (from a Turkish consanguineous family) is homozygous for a region spanning 25 cM region at the *OC116* locus (indicated by boxed haplotypes). A recombination event in family P locates the osteopetrosis region on chromosome 11 proximal to *D11S911*.

## RESULTS

We analyzed 10 patients with infantile malignant osteopetrosis without a positive family history. All but one patient (patient R) had undergone bone marrow transplantation between 2 and 6 months of age. In addition to a severe osteopetrotic bone phenotype and typical hematological abnormalities, all patients with the exception of patient K showed signs of severe visual impairment. Patients M, P, S and T were from consanguineous families and microsatellite analysis revealed homozygosity at the *OC116* locus (data for family P are shown in Fig. 1). Patient R from a consanguineous family from Kuwait was heterozygous at this locus and therefore was excluded from further analyses (Fig. 1). Mutation analysis was performed by sequencing all 19 coding exons after amplification from genomic DNA. We identified *OC116* mutations in five of the nine patients (Table 1). Two independent patients were homozygous for mutations that predict a total loss of function since they truncate the protein within the membrane

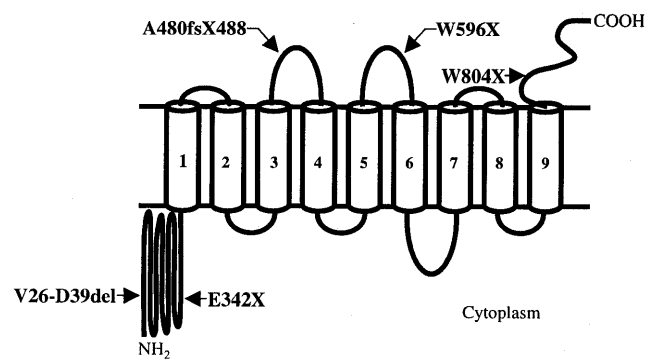


**Figure 2.** Topology model [according to Leng *et al.* (22)] of Vph1p, a yeast homolog of the 116 kDa  $\alpha$ -subunit of the  $H^+$ -ATPase. The locations of mutations (at the amino acid level) found in osteopetrotic patients are indicated by arrows. The corresponding mutations at the DNA level are indicated in Table 1.

spanning block (Fig. 2). In patient M, a 1787G→A point mutation creates a premature stop codon at position 596. In patient T, a homozygous 2 bp deletion in exon 12 (1438–1439del) predicts a premature stop at position 488 after eight extraneous amino acids that are translated from the wrong reading frame. Further, in patient P we detected a homozygous A→T transversion in intron 2 close to a splice site. At this position (+4), T is found in 8% and A in 74% of the cases (21). To detect possible effects on splicing, we extracted RNA from fibroblasts established from patient P and amplified the relevant region by RT-PCR using exonic primers. This revealed the use of a cryptic splice site in the preceding exon (Fig. 3). This deletes 14 amino acids of the N-terminal, intracellular portion of the protein (V26–D39del) (Fig. 2). As expected, all the homozygous mutations are present in both parents in a heterozygous state (data not shown).

In addition, stop mutations on one allele were found in patients B [1024G→T (E342X)] and K [2412G→A (W804X)]. The heterozygous stop mutation is also present in the mother and the brother of patient B, who are both unaffected. This shows that a 50% reduction in gene dosage is not sufficient to cause disease, and suggests the presence of another, still undetected mutation on the second allele of the patient.

The stop codon in patient K was also verified by RT-PCR performed on RNA from leukocytes (data not shown), proving that the mutated transcript is stable and may be translated into a protein lacking the C-terminal 25 amino acids. Since this

**Table 1.** Mutations in five osteopetrotic patients

Patient	Location in DNA	Mutation	Consequence	Location in protein	Allele
B (German family)	Exon 10	1024G→T	E342X	N-terminus	Heterozygous
K (Turkish family)	Exon 20	2412G→A	W804X	C-terminus	Heterozygous
M (German inbred family)	Exon 15	1787G→A	W596X	Loop V/VI	Homozygous
P (Turkish inbred family)	Intron 2	IVS2+4A→T	V26–D39del	N-terminus	Homozygous
T (Turkish inbred family)	Exon 12	1438–1439del	A480fsX488	Loop III/IV	Homozygous

All patients presented with typical symptoms of infantile malignant osteopetrosis (2). All received bone marrow transplantation during the first year of life. Patient K was exceptional in that he showed only moderate visual impairment. Mutations were named according to guidelines given at <http://www.dmd.nl/mutnomen.html>.

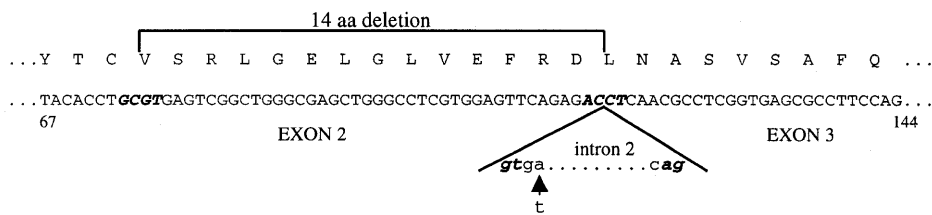


**Figure 3.** Aberrant splicing of intron 2 due to the homozygous IVS2+4A→T mutation in patient P. The cDNA sequence is given in capital letters from position 67 to 144 with amino acid translation above. Positions -2 to +2 of the regular and the cryptic splice donor site and the splice acceptor site are shown in bold and italic. The sequence of the beginning and the end of wild-type intron 2 is given in lower case letters. The arrow indicates the A→T transversion at position +4. Usage of an upstream cryptic donor splice site leads to a deletion of 14 amino acids in-frame as indicated by the bar.

mutation is also present in the mother of the patient, it alone cannot be the cause of the disease. It is likely that the patient is a compound heterozygote and the mutation on the other allele has not been found.

## DISCUSSION

This work identifies the first gene underlying human infantile osteopetrosis. We have found *OC116* mutations in five of ten patients, suggesting that mutations in this gene are a rather common cause of this disease. It also shows that *oc/oc* mice (7) and *Atp6i* knockout mice (20) are realistic animal models for recessive infantile human osteopetrosis. However, the fact that no mutations could be identified in four patients, and that microsatellite analysis did not show homozygosity at the *OC116* locus in a patient from a consanguineous family, suggests that there may be additional genes underlying infantile recessive osteopetrosis in man.

The mutations found in patients M and T almost certainly cause a total loss of  $\alpha 3$  subunit function. Both mutations result in premature stop codons that truncate the protein after the third or fifth predicted transmembrane domain, respectively (Table 1 and Fig. 2). Structure–function studies of the homologous yeast subunit Vph1p have shown that residues in transmembrane domains VIII and IX are important for the pump activity (possibly by participating in the transmembrane path for proton translocation). Furthermore, the extracellular C-terminus may play a role in subunit assembly (22,23).

The splice site mutation in patient P (IVS2+4A→T) results in a deletion of 14 amino acids from the cytoplasmic N-terminus of the protein (Fig. 3). Because the expression of the  $\alpha 3$  subunit is not restricted to osteoclasts (17,24), we could detect this aberrant splicing by analyzing mRNA from fibroblasts established from the patient. Although the function of the N-terminus of this subunit is not known in detail, it has been proposed to interact with the cytoplasmic  $V_1$  part of the proton pump complex (24). This part comprises the subunits A and B that are involved in ATP binding and hydrolysis.

The premature stop codon in patient K truncates the extracellular C-terminus of the  $\alpha 3$  subunit by 25 amino acids. These residues are known to play a role in the assembly of the  $H^+$ -ATPase multisubunit complex (25), again suggesting a loss of function. Although we assume that there is a *OC116* mutation on the second allele of the patient, we have not yet been able to identify it. The fact that the C-terminal stop mutation was heterozygous on the cDNA level implies that both alleles are expressed in leukocytes of the patient. However, leuko-

cytes express a truncated form of *oc-116* named *tirc7* (18). Thus, these results do not exclude the possibility that unidentified mutations are present in the regulatory or intronic regions of *OC116*. Interestingly, patient K had the mildest phenotype among our patients. In contrast to the other patients, his vision was not severely affected even at 2 years of age. It is therefore possible that the mutated  $H^+$ -ATPase has a residual activity. This hypothesis needs further testing.

Osteopetrosis is the second disorder caused by mutations in a V-type  $H^+$ -ATPase subunit. Mutations in the B1 subunit cause renal tubular acidosis and sensorineural deafness, possibly by interfering with apical acid secretion in specialized cell populations in the cochlea and the kidney (26). Mutations in the B1 subunit do not affect osteoclast function because these cells preferentially express the B2 isoform (27). Together with the present work, this highlights the various roles of V-type  $H^+$ -ATPase subunit isoforms. They may differ in tissue distribution, subcellular localization and biochemical properties. Interestingly, there are also two proteins (Vph1p and STV1p) homologous to mammalian  $\alpha$ -subunits in the *Saccharomyces cerevisiae* (15). In yeast, V-ATPases containing these different subunits are targeted to different intracellular compartments, suggesting that the  $\alpha$ -subunit may carry a sorting signal. Indeed, while in *Atp6i* knockout mice osteoclasts failed to acidify extracellular lacunae, they retain acidic lysosomes, and the acidification of intracellular compartments in the liver appeared to be normal (20). Nonetheless, the expression pattern of the  $\alpha 3$  subunit, which is not restricted to osteoclasts, should prompt investigations on whether other symptoms observed in osteopetrotic patients (e.g. visual disturbances and, in some cases, central nervous system symptoms) might be due to intracellular acidification defects in these organs.

## MATERIALS AND METHODS

### DNA and RNA extraction

DNA was isolated from fibroblasts and blood by standard procedures. RNA was isolated from fibroblasts or leukocytes (after lysing erythrocytes) with the Qiagen RNeasy kit (Qiagen, Hilden, Germany) according to the manufacturer's instructions.

### Microsatellite markers

Microsatellite markers flanking the *OC116* locus (*D11S905*, *D11S1313*, *D11S1883*, *D11S4113*, *D11S4136*, *D11S4139*,

**Table 2.** Primers and conditions for exon amplification

Amplified exons	Primer name	Primer sequence (5'→3')	Size of fragment (bp)	PCR
2-3	OC2a	cagtgagtgaaaggcgcacagg	680	a
	OC3r	tgctggaatgtaggcctgg		
4-5	OC4a	cctcaactgttgagacaacctc	535	b
	OC5r	acaaggagtcggagctcagc		
6-7	OC6a	tgccaattgcccattgc	479	a
	OC7r	tggggaggagtcacgatagg		
8-9	OC8a	cagactcagagtctctgtagc	667	a
	OC9r	ctggaagtgaggcagaaacg		
10	OC10a	gctgatcatctccacgtcagag	463	a
	OC10r	cctcacactggctgcagagc		
11-13	OC11a	ggcagatgctggtgtgttcg	674	a
	OC13r	caggacggctgaaccgagg		
14-15	OC14a	ggacttctggcagtgatgg	550	a
	OC15r	tcccagtggccctgtgacc		
16-18	OC16a	ttgcaggtgtgcacagcagg	668	a
	OC18r	cagccgtcggggccagg		
19-20	OC19a	ctggcaggcaccacttgc	472	a
	OC20r	gacgagacatcactgccagg		

<sup>a</sup>Three cycles at 94°C for 1 min, 60°C for 1 min, 68°C for 2 min and 36 cycles at 94°C for 30 s, 57°C for 30 s and 68°C for 1 min.

<sup>b</sup>Three cycles at 94°C for 1 min, 57°C for 1 min, 68°C for 2 min and 36 cycles at 94°C for 30 s, 54°C for 30 s and 68°C for 1 min.

*D11S1314*, *D11S916* and *D11S911*) were amplified in radioactive PCR reactions and analyzed according to standard protocols.

#### Exon amplification, RT-PCR and mutation analysis

The genomic organization of the *OC116* gene has been published (18). Intronic primers for the amplification of the 19 coding exons were deduced from the genomic clone under GenBank accession no. AC034259 (Table 2). Amplification of the 19 exons in 9 fragments was performed by PCR using Elongase (Gibco BRL, Gaithersburg, MD) using two different PCR conditions as specified in Table 2.

To amplify cDNA fragments, RNA from fibroblasts or leukocytes was reverse transcribed using Superscript RT-II (Gibco BRL) and random hexamers as primers. The *OC116* cDNA was amplified in two overlapping fragments using the primer pairs OCe1fb (5'-gagcgcggcgcgcagcacac-3')/OCe11r (5'-ggcgaagaggaacatgagcag-3') and OCe10f (5'-catccgacacaccgcttcac-3')/OC20r (5'-gacgagacatcactgccagg-3'), yielding 1276 and 1520 bp fragments, respectively. PCR conditions were identical to those in footnote a in Table 2, but 3% DMSO was added to the reactions containing OCe1fb/OCe11r. The PCR products were purified and directly sequenced on ABI 377 or ABI 310 automated sequencers (Perkin Elmer Applied Biosystems, Foster City, CA) using the BigDye terminator sequencing kit (Perkin Elmer). Sequences were aligned using the MACAW program (Greg Schuler, NCBI, Bethesda, MD).

#### ACKNOWLEDGEMENTS

We thank Gudrun Weets for excellent technical assistance, and the patients for their collaboration. This work was supported by grants from the Deutsche Forschungsgemeinschaft and the Fonds der Chemischen Industrie to T.J.J., and from BONFOR to C.K.

#### REFERENCES

1. Thompson, D.A., Kriss, A., Taylor, D., Russell-Eggitt, I., Hodgkins, P., Morgan, G., Vellodi, A. and Gerritsen, E.J. (1998) Early VEP and ERG evidence of visual dysfunction in autosomal recessive osteopetrosis. *Neuropediatrics*, **29**, 137-144.
2. Gerritsen, E.J., Vossen, J.M., van Loo, I.H., Hermans, J., Helfrich, M.H., Griscelli, C. and Fischer, A. (1994) Autosomal recessive osteopetrosis: variability of findings at diagnosis and during the natural course. *Pediatrics*, **93**, 247-253.
3. Keith, C.G. (1968) Retinal atrophy in osteopetrosis. *Arch. Ophthalmol.*, **79**, 234-241.
4. Gerritsen, E.J., Vossen, J.M., Fasth, A., Friedrich, W., Morgan, G., Padmos, A., Vellodi, A., Porras, O., O'Meara, A., Porta, F. *et al.* (1994) Bone marrow transplantation for autosomal recessive osteopetrosis. A report from the Working Party on Inborn Errors of the European Bone Marrow Transplantation Group. *J. Pediatr.*, **125**, 896-902.
5. Yoshida, H., Hayashi, S., Kunisada, T., Ogawa, M., Nishikawa, S., Okamura, H., Sudo, T. and Shultz, L.D. (1990) The murine mutation osteopetrosis is in the coding region of the macrophage colony stimulating factor gene. *Nature*, **345**, 442-444.
6. Soriano, P., Montgomery, C., Geske, R. and Bradley, A. (1991) Targeted disruption of the *c-src* proto-oncogene leads to osteopetrosis in mice. *Cell*, **64**, 693-702.

7. Scimeca, J.C., Franchi, A., Trojani, C., Parrinello, H., Grosgeorge, J., Robert, C., Jaillon, O., Poirier, C., Gaudray, P. and Carle, G.F. (2000) The gene encoding the mouse homologue of the human osteoclast-specific 116-kDa V-ATPase subunit bears a deletion in osteosclerotic (oc/oc) mutants. *Bone*, **26**, 207–213.
8. Lazner, F., Gowen, M., Pavasovic, D. and Kola, I. (1999) Osteopetrosis and osteoporosis: two sides of the same coin. *Hum. Mol. Genet.*, **8**, 1839–1846.
9. Roth, D.E., Venta, P.J., Tashian, R.E. and Sly, W.S. (1992) Molecular basis of human carbonic anhydrase II deficiency. *Proc. Natl Acad. Sci. USA*, **89**, 1804–1808.
10. Lowe, C., Yoneda, T., Boyce, B.F., Chen, H., Mundy, G.R. and Soriano, P. (1993) Osteopetrosis in Src-deficient mice is due to an autonomous defect of osteoclasts. *Proc. Natl Acad. Sci. USA*, **90**, 4485–4489.
11. Trubert, C.L., Bernard, F., Hivroz, C., Carlizo, A., Fischer, A. and Cournot, G. (1997) PP60c-src expression in osteoclasts from osteopetrotic children and in giant tumor cells. *Eur. J. Histochem.*, **41**, 169–176.
12. Orchard, P.J., Dahl, N., Aukerman, S.L., Blazar, B.R. and Key Jr, L.L. (1992) Circulating macrophage colony-stimulating factor is not reduced in malignant osteopetrosis. *Exp. Hematol.*, **20**, 103–105.
13. Baron, R., Neff, L., Louvard, D. and Courtoy, P.J. (1985) Cell-mediated extracellular acidification and bone resorption: evidence for a low pH in resorbing lacunae and localization of a 100-kD lysosomal membrane protein at the osteoclast ruffled border. *J. Cell Biol.*, **101**, 2210–2222.
14. Blair, H.C. (1998) How the osteoclast degrades bone. *Bioessays*, **20**, 837–846.
15. Forgac, M. (1999) Structure and properties of the vacuolar H<sup>+</sup>-ATPases. *J. Biol. Chem.*, **274**, 12951–12954.
16. Li, Y.P., Chen, W. and Stashenko, P. (1996) Molecular cloning and characterization of a putative novel human osteoclast-specific 116-kDa vacuolar proton pump subunit. *Biochem. Biophys. Res. Commun.*, **218**, 813–821.
17. Toyomura, T., Oka, T., Yamaguchi, C., Wada, Y. and Futai, M. (2000) Three subunit isoforms of mouse vacuolar H<sup>+</sup>-ATPase. Preferential expression of the  $\alpha 3$  isoform during osteoclast differentiation. *J. Biol. Chem.*, **275**, 8760–8765.
18. Heinemann, T., Bulwin, G.C., Randall, J., Schnieders, B., Sandhoff, K., Volk, H.D., Milford, E., Gullans, S.R. and Utku, N. (1999) Genomic organization of the gene coding for TIRC7, a novel membrane protein essential for T cell activation. *Genomics*, **57**, 398–406.
19. Heaney, C., Shalev, H., Elbedour, K., Carmi, R., Staack, J.B., Sheffield, V.C. and Beier, D.R. (1998) Human autosomal recessive osteopetrosis maps to 11q13, a position predicted by comparative mapping of the murine osteosclerosis (oc) mutation. *Hum. Mol. Genet.*, **7**, 1407–1410.
20. Li, Y.P., Chen, W., Liang, Y., Li, E. and Stashenko, P. (1999) *Atp6i*-deficient mice exhibit severe osteopetrosis due to loss of osteoclast-mediated extracellular acidification. *Nature Genet.*, **23**, 447–451.
21. Senapathy, P., Shapiro, M.B. and Harris, N.L. (1990) Splice junctions, branch point sites, and exons: sequence statistics, identification, and applications to genome project. *Methods Enzymol.*, **183**, 252–278.
22. Leng, X.H., Nishi, T. and Forgac, M. (1999) Transmembrane topography of the 100-kDa a subunit (Vph1p) of the yeast vacuolar proton-translocating ATPase. *J. Biol. Chem.*, **274**, 14655–14661.
23. Leng, X.H., Manolson, M.F., Liu, Q. and Forgac, M. (1996) Site-directed mutagenesis of the 100-kDa subunit (Vph1p) of the yeast vacuolar H<sup>+</sup>-ATPase. *J. Biol. Chem.*, **271**, 22487–22493. [Erratum (1996) *J. Biol. Chem.*, **271**, 28725.]
24. Nishi, T. and Forgac, M. (2000) Molecular cloning and expression of three isoforms of the 100-kDa a subunit of the mouse vacuolar proton-translocating ATPase. *J. Biol. Chem.*, **275**, 6824–6830.
25. Leng, X.H., Manolson, M.F. and Forgac, M. (1998) Function of the COOH-terminal domain of Vph1p in activity and assembly of the yeast V-ATPase. *J. Biol. Chem.*, **273**, 6717–6723.
26. Karet, F.E., Finberg, K.E., Nelson, R.D., Nayir, A., Mocan, H., Sanjad, S.A., Rodriguez-Soriano, J., Santos, F., Cremers, C.W., Di Pietro, A. *et al.* (1999) Mutations in the gene encoding B1 subunit of H<sup>+</sup>-ATPase cause renal tubular acidosis with sensorineural deafness. *Nature Genet.*, **21**, 84–90.
27. Mattsson, J.P., Skyman, C., Palokangas, H., Vaananen, K.H. and Keeling, D.J. (1997) Characterization and cellular distribution of the osteoclast ruffled membrane vacuolar H<sup>+</sup>-ATPase B-subunit using isoform-specific antibodies. *J. Bone Miner. Res.*, **12**, 753–760.
28. Dib, C., Faure, S., Fizames, C., Samson, D., Drouot, N., Vignal, A., Millasseau, P., Marc, S., Hazan, J., Seboun, E. *et al.* (1996) A comprehensive genetic map of the human genome based on 5,264 microsatellites. *Nature*, **380**, 152–154.

